

NATIONAL ADVISORY COMMITTEE FOR AERONAUTICS

TECHNICAL NOTE 4200

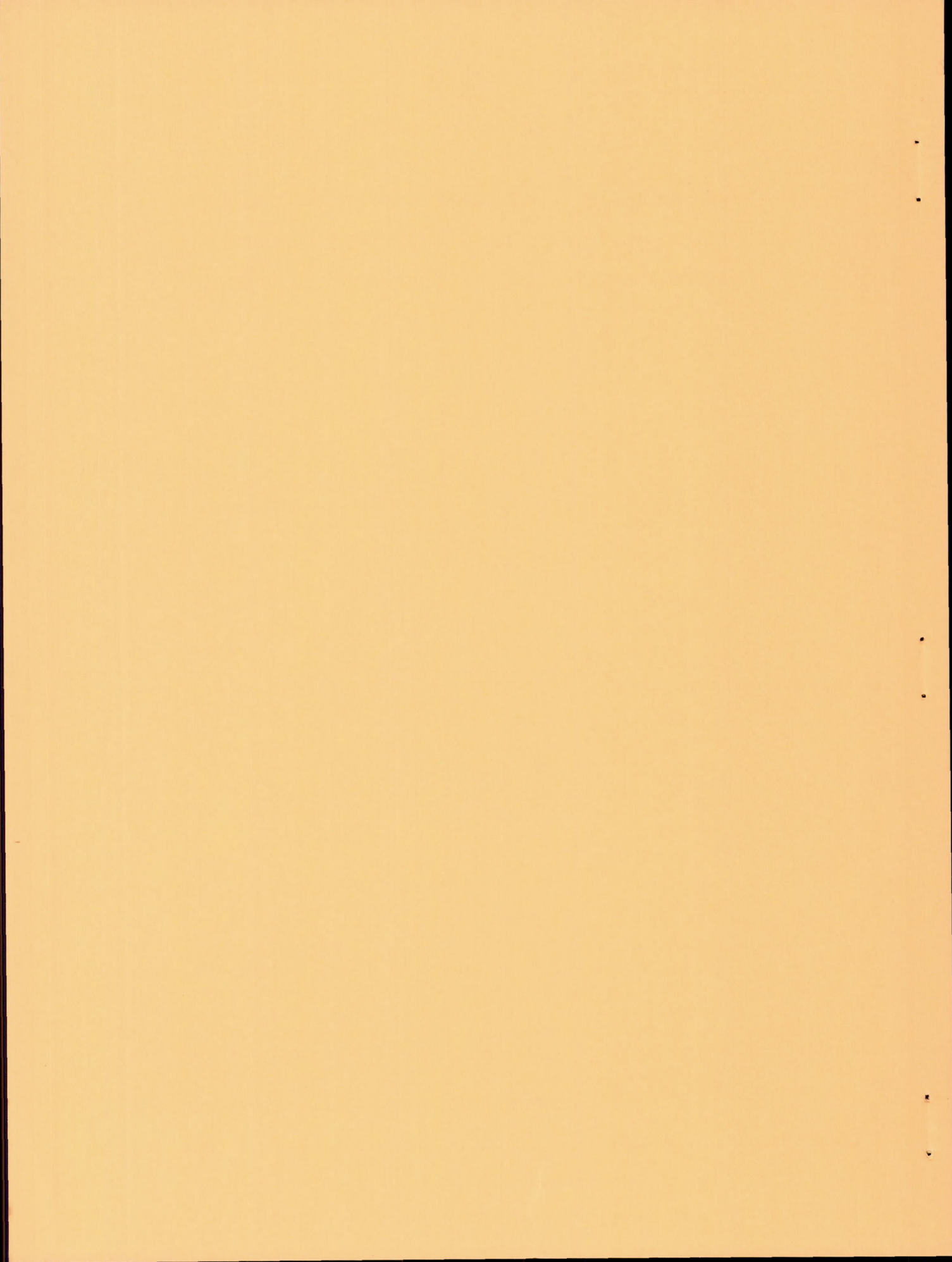
EFFECTIVENESS OF BOUNDARY-LAYER CONTROL, OBTAINED BY
BLOWING OVER A PLAIN REAR FLAP IN COMBINATION WITH
A FORWARD SLOTTED FLAP, IN DEFLECTING A SLIPSTREAM
DOWNWARD FOR VERTICAL TAKE-OFF

By Kenneth P. Spreemann

Langley Aeronautical Laboratory
Langley Field, Va.



Washington
February 1958



NATIONAL ADVISORY COMMITTEE FOR AERONAUTICS

TECHNICAL NOTE 4200

EFFECTIVENESS OF BOUNDARY-LAYER CONTROL, OBTAINED BY
BLOWING OVER A PLAIN REAR FLAP IN COMBINATION WITH
A FORWARD SLOTTED FLAP, IN DEFLECTING A SLIPSTREAM
DOWNWARD FOR VERTICAL TAKE-OFF

By Kenneth P. Spreemann

SUMMARY

An investigation of the effectiveness of boundary-layer control, obtained by blowing a jet sheet of air over a plain rear flap in combination with a forward slotted flap, in deflecting a propeller slipstream downward for vertical take-off has been conducted in a static-thrust facility at the Langley Aeronautical Laboratory. The investigation indicated that the plain rear flap alone with a low momentum coefficient for boundary-layer control provided larger turning angles than the combined slotted and plain flaps without boundary-layer control. Within the region of ground effects the configuration of this investigation manifested reductions in turning angle and ratio of resultant force to thrust that were similar to those shown for numerous configurations of previous investigations with or without boundary-layer control.

The slotted and plain flap of this investigation (with boundary-layer control over the rear flap) provided larger turning angles and ratios of resultant force to thrust than the double plain flap configuration of a previous investigation (with boundary-layer control over the forward flap).

INTRODUCTION

An investigation of various wing-flap configurations has been conducted at the Langley Laboratory in an effort to develop simple arrangements capable of deflecting the propeller slipstream downward for vertical take-off. The capabilities of some of these configurations are reported in references 1 to 6. The effect of blowing boundary-layer control on the ability of a wing to deflect the slipstream was investigated in references 5 and 6. In these studies boundary-layer control was applied at

the knee of the first flap. Experience has shown, however, that flow separation is most likely to occur on the second flap. Therefore, an exploratory investigation was undertaken to determine the slipstream deflection characteristics of a wing with blowing boundary-layer control applied only to the second flap. The investigation was conducted in a static-thrust facility and employed a model wing equipped with a 67-percent-chord slotted forward flap and a 33-percent-chord plain rear flap. A full-span blowing nozzle was located at the trailing edge of the forward flap for applying boundary-layer control to the rear flap.

COEFFICIENTS AND SYMBOLS

The positive sense of forces, moments, and angles used in this paper is indicated in figure 1. Moments are referred to the quarter-chord point of the mean aerodynamic chord.

$b/2$	wing semispan, ft
c	wing chord, ft
D	propeller diameter, ft
h	height of wing trailing edge above ground, ft
$\delta_{f,1}$	deflection of forward or slotted flap relative to wing chord, deg
$\delta_{f,2}$	deflection of rear or plain flap relative to slotted-flap chord, deg
L	lift, lb
F_X	longitudinal force (thrust minus drag), lb
M	pitching moment, ft-lb
F	resultant force, lb
T	propeller thrust, 15 lb
θ	turning angle, inclination of resultant-force vector from thrust axis, $\tan^{-1} \frac{L}{F_X}$, deg
C_μ''	momentum coefficient, $\frac{Q_n \rho_n V_n}{q'' S}$

C_q''	flow coefficient, $\frac{Q_n}{V''S}$
C_p''	pressure coefficient, $\frac{p - p''}{q''}$
P	power in blowing system, $\frac{\rho_n \frac{t}{12} \frac{b}{2} (v_n)^3}{2}$, ft-lb/sec
P''	power in slipstream, $\frac{\rho'' \frac{\pi D^2}{4} (V'')^3}{4}$, ft-lb/sec
Q_n	quantity of air blown out of nozzle expanded to slipstream static pressure, cu ft/sec
ρ_n	mass density of air blown out of nozzle, slugs/cu ft
V_n	nozzle exit velocity, isentropic expansion to slipstream static pressure being assumed, ft/sec
ρ''	mass density of air in slipstream, slugs/cu ft
V''	slipstream velocity, ft/sec
q''	slipstream dynamic pressure, $\frac{T}{\pi D^2/4}$, lb/sq ft
S	wing area of semispan model, sq ft
p	static pressure in blowing system, lb/sq ft
p''	slipstream static pressure, lb/sq ft
t	effective nozzle gap, in.

APPARATUS AND METHOD

A drawing of the model, with pertinent dimensions, is presented in figure 2, and a photograph of the model mounted for testing is shown in figure 3. The geometric characteristics of the model are given in the following table:

Wing:

Area (semispan), sq ft	3.0
Span (semispan), ft	2.0
Chord, ft	1.5
Aspect ratio	2.67
Taper ratio	1.0
Airfoil section (approximate)	NACA 4412

Propeller:

Diameter, ft	2.0
Nacelle diameter, ft	0.33
Airfoil section	Clark Y
Solidity	0.07

The model was made up by using the wing which was employed in reference 6 as the flap of the present model. A new leading-edge section was added to increase the total chord to 18 inches. This combination resulted in a 12-percent-thick airfoil section.

The profile of the forward slotted flap approximated that of the slotted flap 2-h of reference 7. The leading part of the wing and the slotted flap were attached together by external brackets as shown in figure 3. With the slotted flap deflected, the gap between the trailing edge of the fixed part of the wing and the nearest point on the leading edge of the flap was held constant at $0.014c$ for all flap angles. (See fig. 2.) The plain rear flap was hinged at 67 percent of the wing chord.

The slotted flap contained the plenum chamber and blowing nozzle. The plenum chamber extended through the wing root and terminated in a plate which served as a base for mounting the model on the balance. Air was exhausted through the nozzle over the plain rear flap. (See fig. 2.) The full-span nozzle, employed for boundary-layer control, had an effective nozzle gap of 0.017 inch.

The flow coefficient, pressure coefficient, and ratio of power in blowing system to power in the slipstream are plotted against momentum coefficient in figure 4. The mass flow through the nozzle was measured by means of a standard sharp-edge-orifice flowmeter. Air was supplied through a 1/2-inch line at 90 pounds per square inch.

For these tests the propeller was mounted independently as shown in figures 2 and 3. The propeller was driven by a variable-frequency electric motor at about 5,500 revolutions per minute, which gave a tip Mach number of approximately 0.52. The motor was mounted inside an aluminum-alloy nacelle by means of strain-gage beams in such a way that the propeller thrust and torque could be measured. The total lift, longitudinal force, and pitching moment of the model were measured on a strain-gage balance located at the root of the wing.

The ground was simulated by a sheet of plywood as shown in figure 1. The ground board extended about 2 feet in front, 3 feet behind, and 2 feet beyond the wing tip of the model. All tests with the ground board were conducted with an angle of 20° between the ground board and thrust axis of the propeller.

The investigation was conducted in a static-thrust facility at the Langley Aeronautical Laboratory. All data presented were obtained at zero forward velocity with a thrust of 15 pounds from the propeller. Inasmuch as these tests were conducted under static conditions in a large room, none of the corrections that are normally applicable to wind-tunnel tests were employed.

RESULTS AND DISCUSSION

The results of the static tests of this investigation to determine the pitching moments, ratio of resultant force to thrust, turning angles, and power required in the blowing system for various flap deflections are presented in figures 5 to 8 for configurations away from the ground. Figures 9 to 12 show results for configurations within the region of ground effects. The effects of the combined flaps and the plain rear flap alone on the turning angle, ratio of resultant force to thrust, and diving moments for different momentum coefficients are summarized in figure 13. The values of F/T and θ presented in figure 13 were obtained from figures 5 to 8 by selecting the largest value of F/T at a specific turning angle for the particular value of C_μ desired. In figure 14 the envelopes of the variation of F/T with θ and the diving moments for the model of this investigation are compared with those for the plain-flapped model (with blowing over the forward flap) of reference 6. A representative plot of the effects of height above ground on θ and F/T for the model with $\delta_{f,1} = 40^\circ$ and $\delta_{f,2} = 40^\circ$ obtained from figure 10 is shown in figure 15. The variation with height above ground of the pitching moment, ratio of resultant force to thrust, and momentum coefficient required to maintain a constant turning angle of 50° , taken from figure 11, is shown in figure 16.

The momentum coefficients in this investigation are based on the calculated mass flow rather than on the mass flow determined from the measured thrust. For this configuration the measured thrust was 20 to 25 percent lower than the calculated thrust indicated by the flowmeter. These losses may be attributed in part to skin friction over the flap as well as to losses in the nozzle.

Effects of Flap Deflection and Boundary-Layer Control

The summary data of figure 13(a), giving the envelopes of the variation of F/T with θ , show that below the stall the increases in F/T for the model with boundary-layer control compared with the data for the model without boundary-layer control are about equal to the thrust developed by the nozzle (for $C_\mu'' = 0.043$ the measured value of $\Delta F/T$ is 0.041; the calculated value of $\Delta F/T = C_\mu'' \frac{S}{\pi D^2/4} = 0.042$). In this

figure it can also be seen that the plain rear flap alone with a low momentum coefficient for boundary-layer control provided larger turning angles and ratio of resultant force to thrust than the combined slotted and plain flaps without boundary-layer control.

In figure 13(b) it is seen that without boundary-layer control the combined slotted and plain flaps incurred greater diving moments than the single rear flap; these increases in diving moments can be associated with the increases in θ , F/T , and movement of the flap system rearward when the forward flap is deflected.

From the comparison in figure 14 it is seen that the slotted and plain flaps of this investigation with blowing over the rear flap provided larger turning angles and ratios of resultant force to thrust than the double plain flap configuration of reference 6 with blowing over the forward flap. The relative merit of boundary-layer control on the first or second flap segment is difficult to determine from the comparison plot of figure 14 since the double-slotted-flap arrangement had considerably larger values of θ and F/T for the zero C_μ'' case. The increments of F/T and θ produced by boundary-layer control in the two cases appear to be generally about equal.

Effects of Proximity to Ground

Previous work (refs. 3 to 5) has indicated that the reductions in F/T and θ near the ground for a deflected slipstream were partially due to rear flap separation. It was, therefore, hoped that, by the application of boundary-layer control to the rear flap, this separation could be suppressed and these undesirable ground effects relieved. The data of figures 9 to 12 and the summary data of turning effectiveness in figure 15 indicate that this condition cannot be realized with a fixed C_μ'' setting. Boundary-layer control provided overall increases in turning effectiveness within and out of the region of ground effects. Within the region of ground effects, however, the action of the jet sheet impinging on the ground apparently causes more of the slipstream to pass over the top of the wing and results in a loss in θ and F/T near the ground. (See fig. 15.) This action has been fully discussed in reference 3.

A study of figures 9 to 12 indicates that by suitable scheduling of C_{μ}'' the effect of the ground on θ can be eliminated and F/T can be increased as the ground is approached. Figure 16 illustrates how C_{μ}'' would have to be scheduled in order to maintain a constant turning angle of 50° . There is the possibility, however, that the power required for such a system might be relatively large very near the ground for some airplane applications. For example, in figure 16 it is seen that a value of h/D of 0.1 requires a value of C_{μ}'' of 0.09 in order to maintain a constant turning angle. The data of figure 4 indicate that, in order to provide a value of C_{μ}'' of 0.09, a ratio of power in the blowing system to power in the slipstream of about 0.30 is required.

CONCLUSIONS

An investigation of the effectiveness of boundary-layer control, obtained by blowing a jet sheet of air over a plain rear flap in combination with a forward slotted flap, in deflecting a propeller slipstream downward for vertical take-off indicated the following conclusions:

1. The plain rear flap alone with a low momentum coefficient for boundary-layer control provided larger turning angles than the combined slotted and plain flap without boundary-layer control.
2. The configuration of this investigation manifested about the same critical range near the ground as was shown for numerous configurations of other investigations with or without boundary-layer control.
3. The slotted and plain flaps of this investigation (with boundary-layer control over the rear flap) provided larger turning angles and ratios of resultant force to thrust than the double plain flap configuration of a previous investigation (with boundary-layer control over the forward flap).

Langley Aeronautical Laboratory,
National Advisory Committee for Aeronautics,
Langley Field, Va., November 12, 1957.

REFERENCES

1. Kuhn, Richard E., and Draper, John W.: An Investigation of a Wing-Propeller Configuration Employing Large-Chord Plain Flaps and Large-Diameter Propellers for Low-Speed Flight and Vertical Take-Off. NACA TN 3307, 1954.
2. Kuhn, Richard E., and Draper, John W.: Investigation of Effectiveness of Large-Chord Slotted Flaps in Deflecting Propeller Slipstreams Downward for Vertical Take-Off and Low-Speed Flight. NACA TN 3364, 1955.
3. Kuhn, Richard E.: Investigation of the Effects of Ground Proximity and Propeller Position on the Effectiveness of a Wing With Large-Chord Slotted Flaps in Redirecting Propeller Slipstreams Downward for Vertical Take-Off. NACA TN 3629, 1956.
4. Kuhn, Richard E., and Spreemann, Kenneth P.: Preliminary Investigation of the Effectiveness of a Sliding Flap in Deflecting a Propeller Slipstream Downward for Vertical Take-Off. NACA TN 3693, 1956.
5. Spreemann, Kenneth P., and Kuhn, Richard E.: Investigation of the Effectiveness of Boundary-Layer Control by Blowing Over a Combination of Sliding and Plain Flaps in Deflecting a Propeller Slipstream Downward for Vertical Take-Off. NACA TN 3904, 1956.
6. Spreemann, Kenneth P.: Investigation of the Effects of Propeller Diameter on the Ability of a Flapped Wing, With and Without Boundary-Layer Control, To Deflect a Propeller Slipstream Downward for Vertical Take-Off. NACA TN 4181, 1957.
7. Wenzinger, Carl J., and Harris, Thomas A.: Wind-Tunnel Investigation of an N.A.C.A. 23012 Airfoil With Various Arrangements of Slotted Flaps. NACA Rep. 664, 1939.

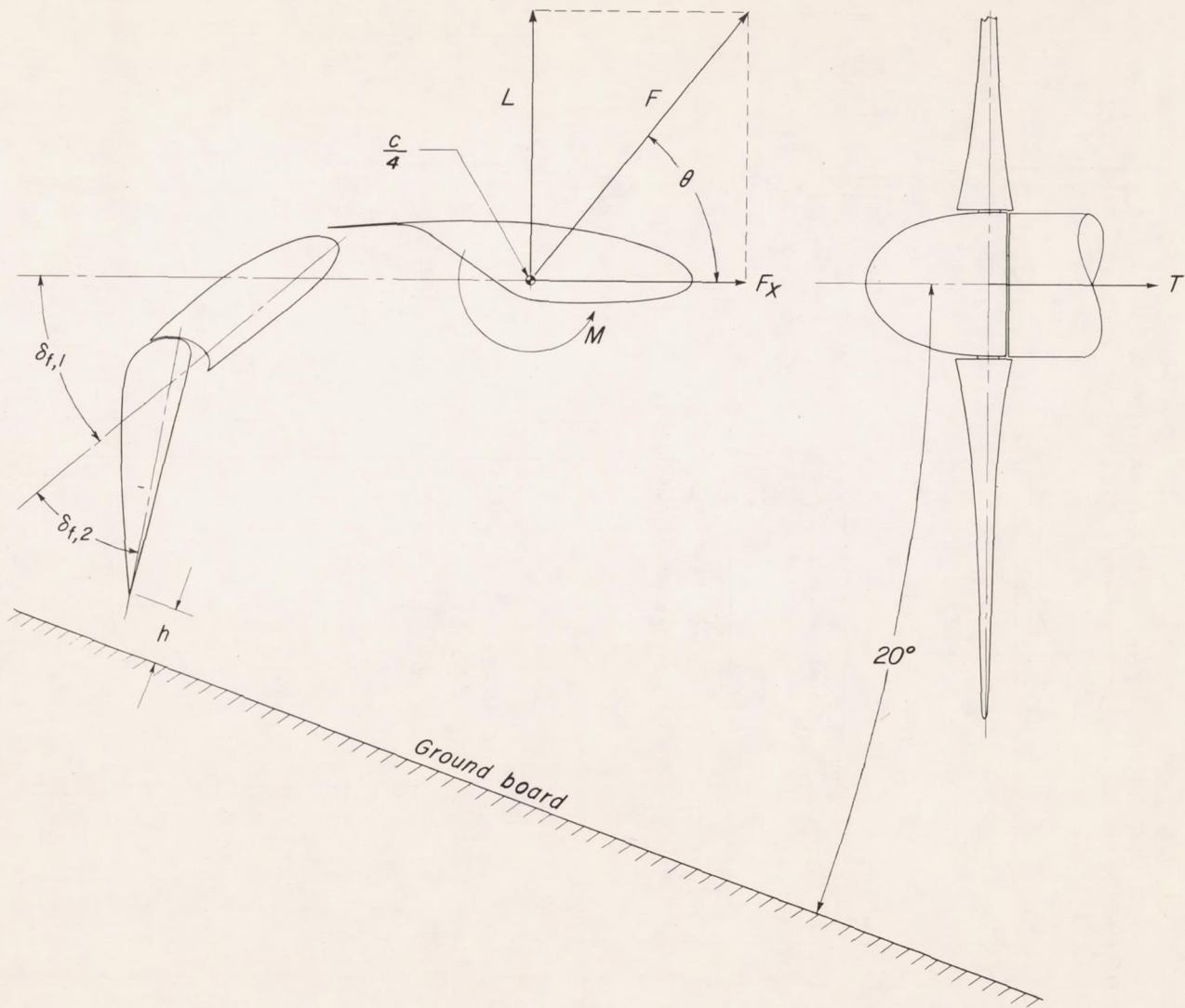


Figure 1.- Conventions used to define positive sense of forces, moments, and angles.

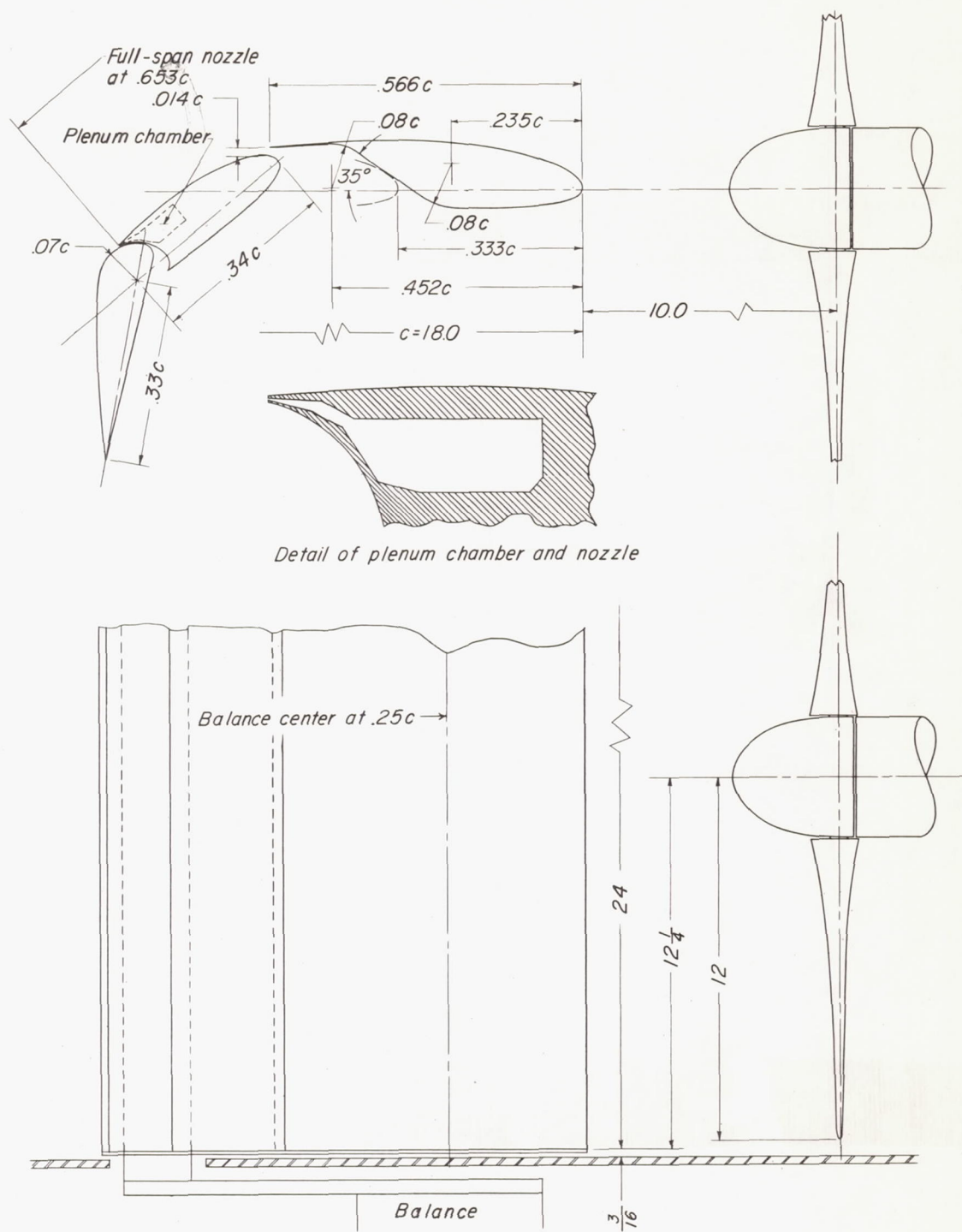


Figure 2.- Drawing of model. All dimensions are in inches.

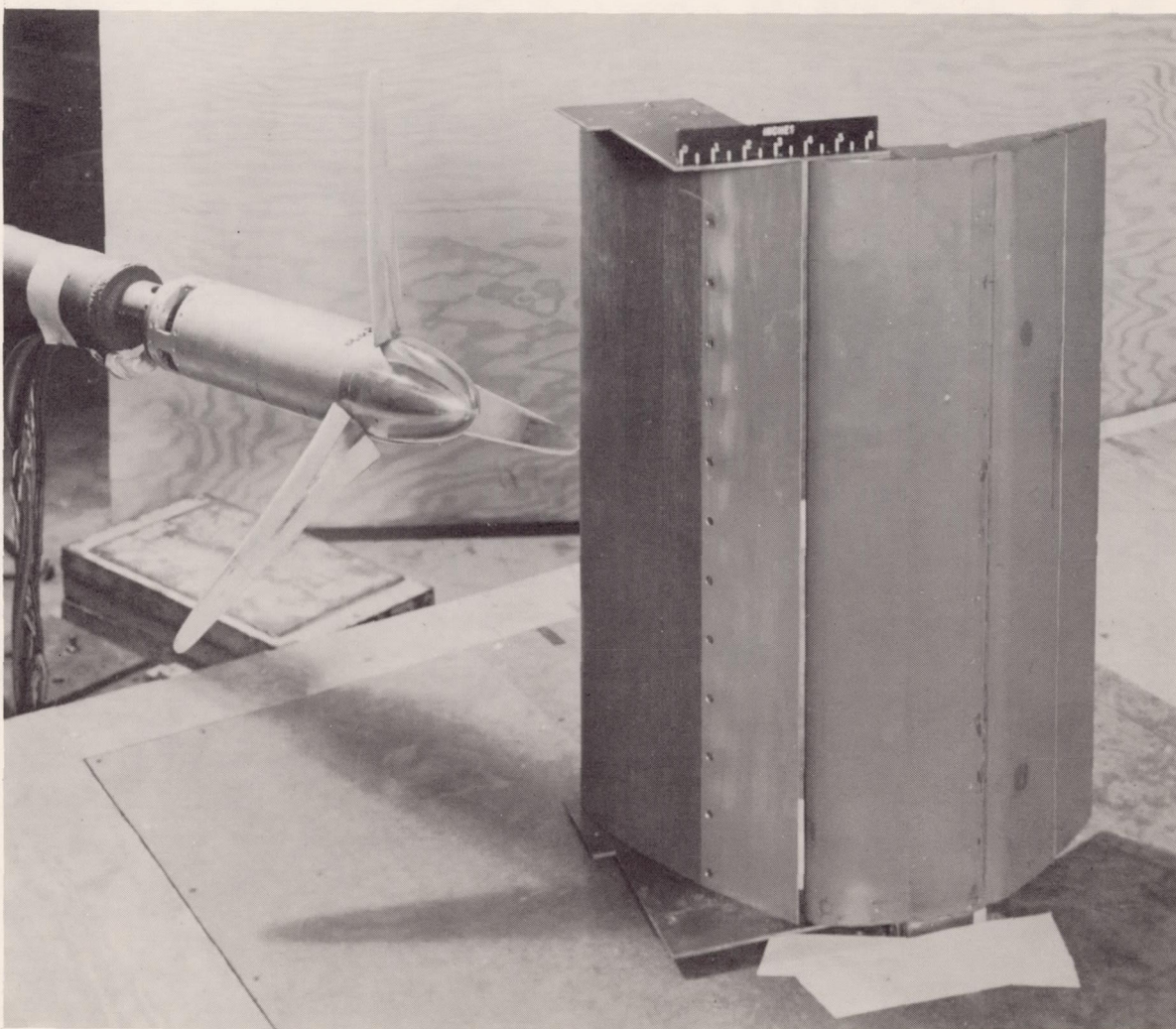
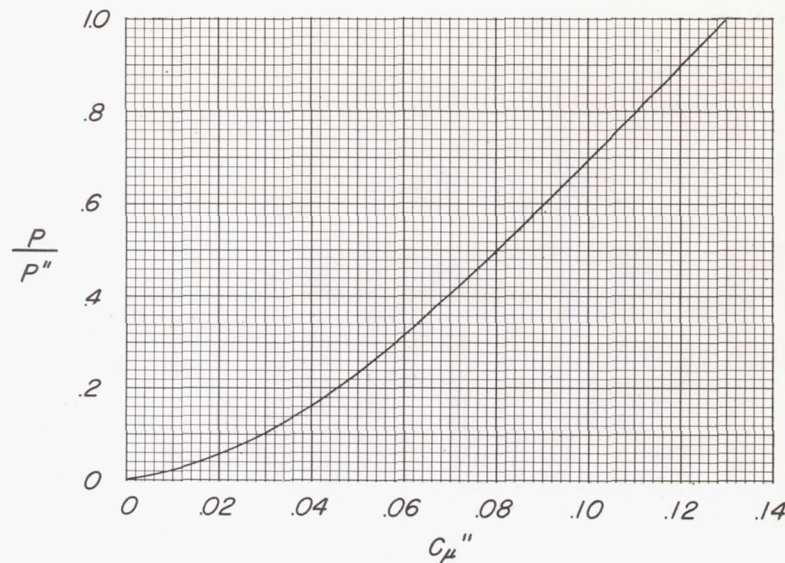
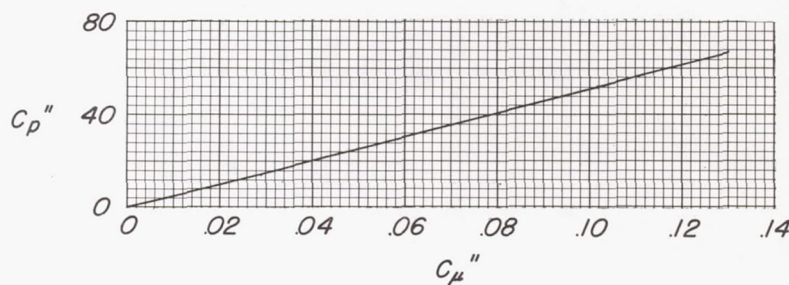


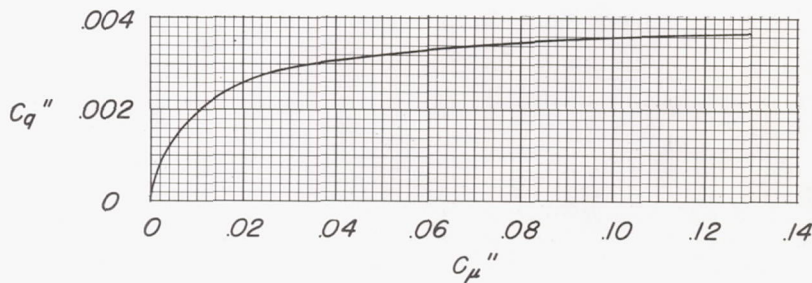
Figure 3.- Model installed on static-thrust stand. L-93299



(a) Ratio of power in blowing system to power in slipstream.

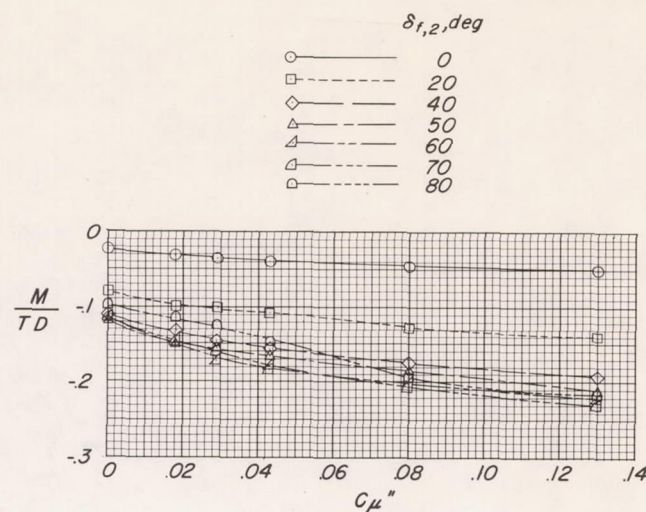


(b) Pressure coefficient.

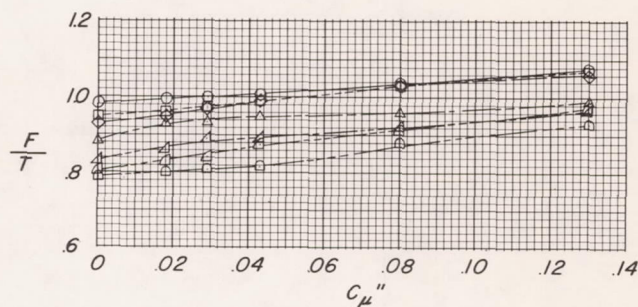


(c) Flow coefficient.

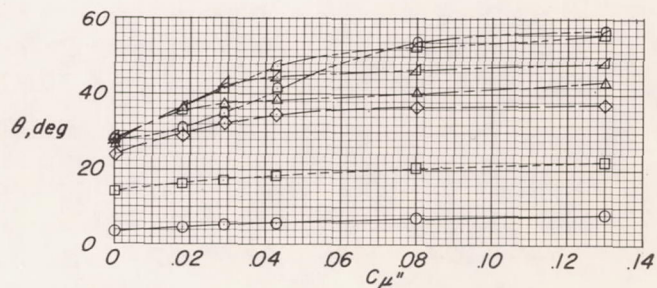
Figure 4.- Variation of ratio of power in blowing system to power in slipstream, pressure coefficient, and flow coefficient with momentum coefficient for 0.017-inch nozzle employed.



(a) Pitching moment.

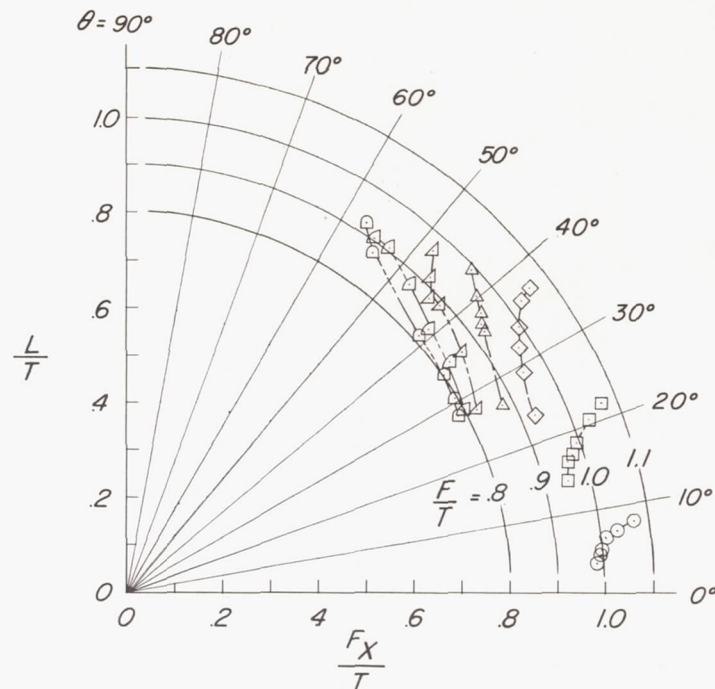


(b) Ratio of resultant force to thrust.

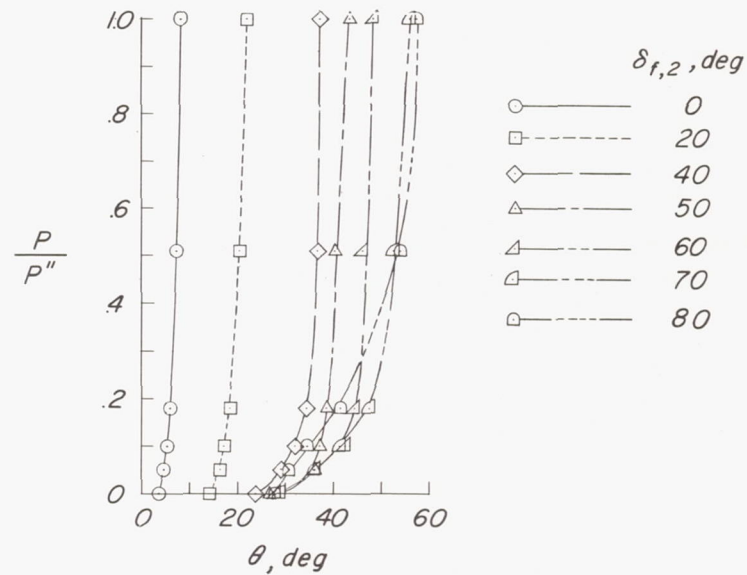


(c) Turning angle.

Figure 5.- Effect of blowing over the flap with $\delta_{f,1}$ constant at 0° on the model characteristics. $h/D \approx \infty$.

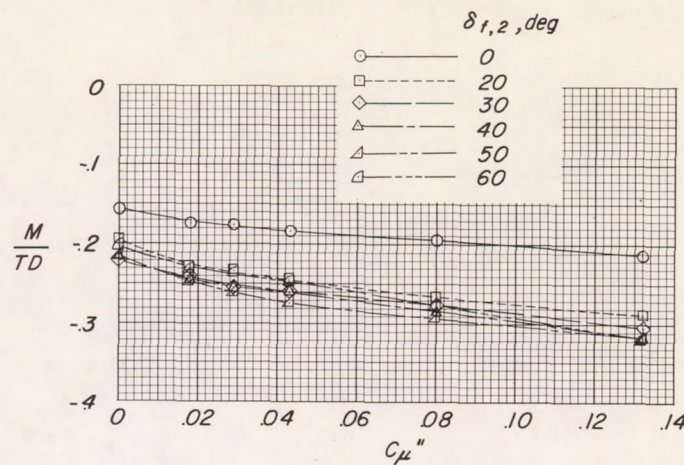


(d) Summary of turning effectiveness.

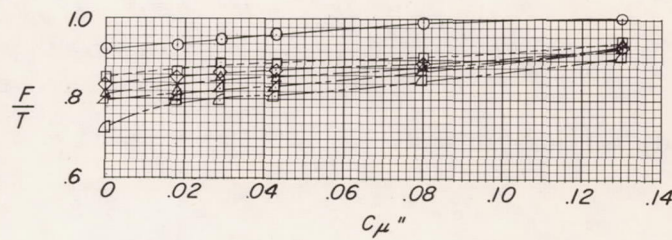


(e) Variation of ratio of power in blowing system to power in slipstream with turning angle.

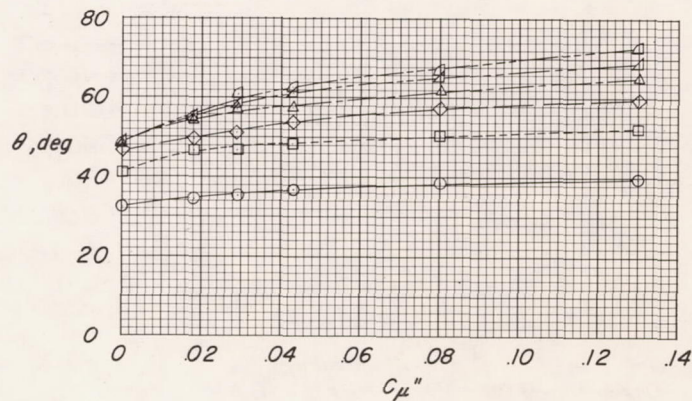
Figure 5.- Concluded.



(a) Pitching moment.

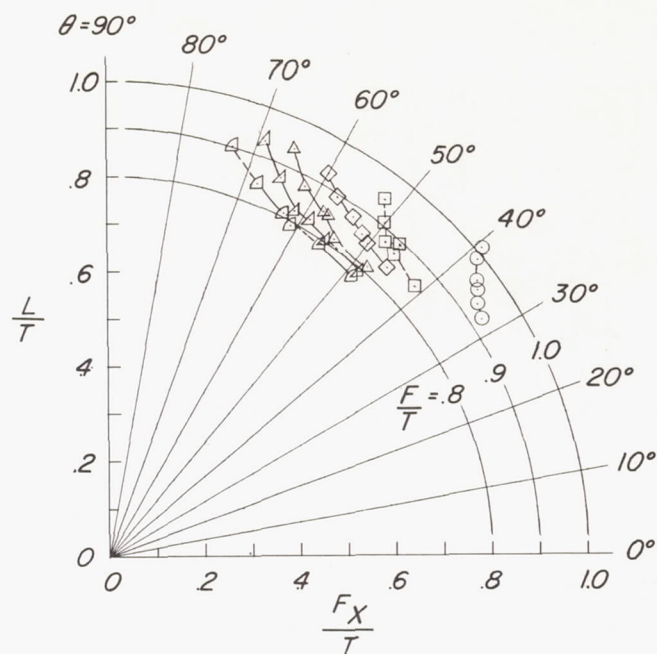


(b) Ratio of resultant force to thrust.

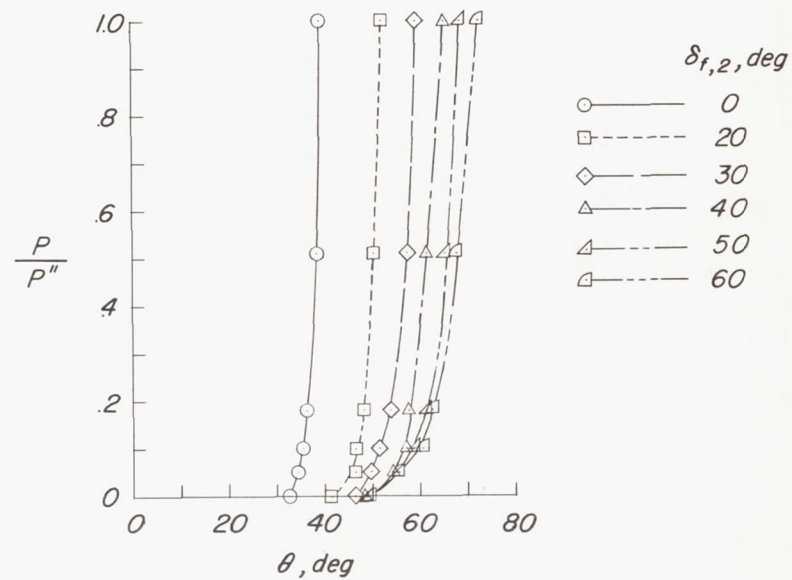


(c) Turning angle.

Figure 6.- Effect of blowing over the flap with $\delta_{f,1}$ constant at 40° on the model characteristics. $h/D \approx \infty$.

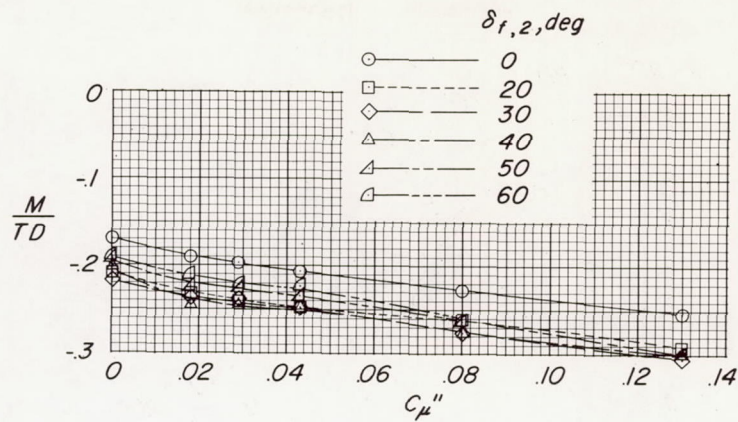


(d) Summary of turning effectiveness.

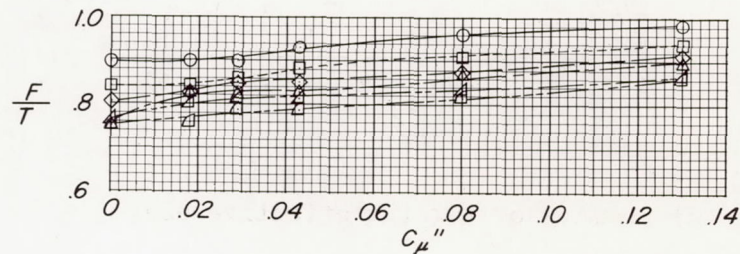


(e) Variation of ratio of power in blowing system to power in slipstream with turning angle.

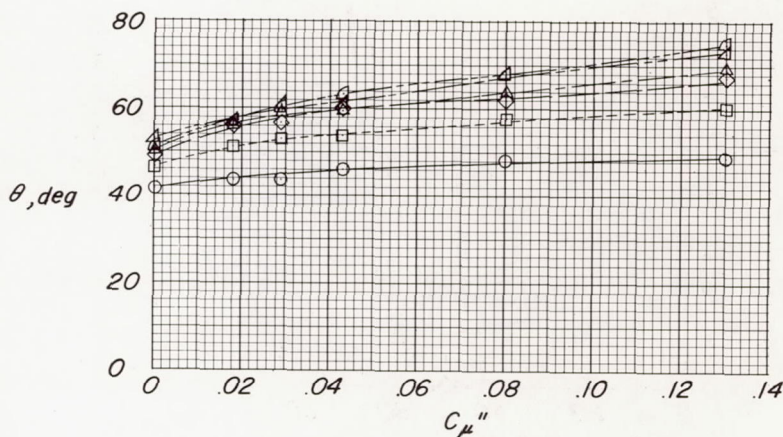
Figure 6.- Concluded.



(a) Pitching moment.

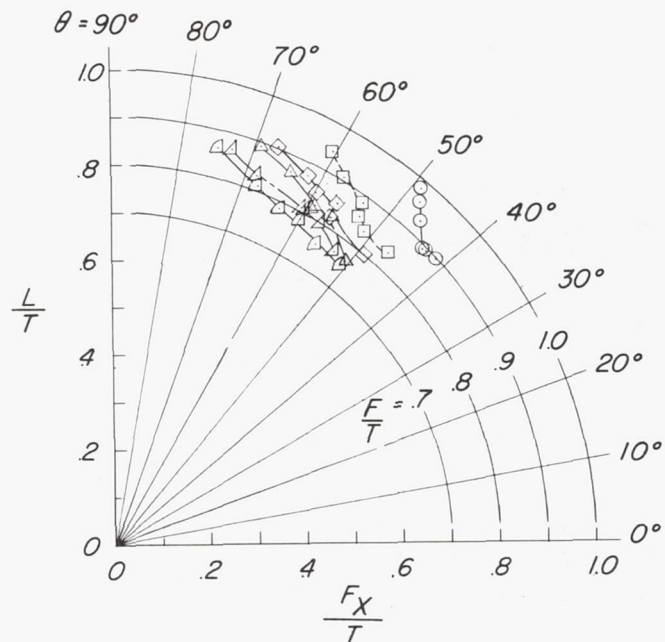


(b) Ratio of resultant force to thrust.

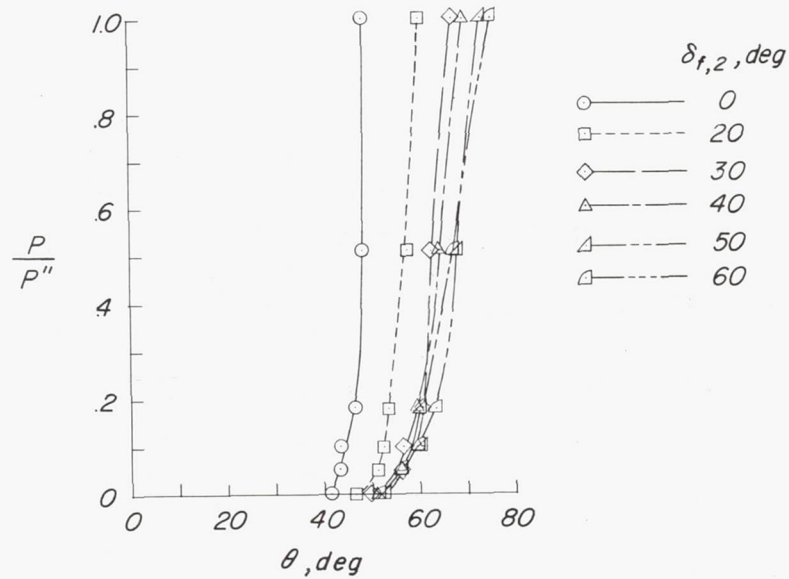


(c) Turning angle.

Figure 7.- Effect of blowing over the flap with $\delta_{f,1}$ constant at 50° on the model characteristics. $h/D \approx \infty$.

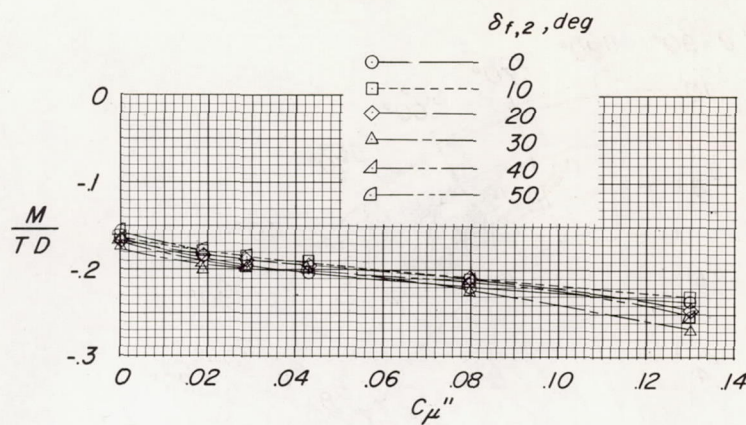


(d) Summary of turning effectiveness.

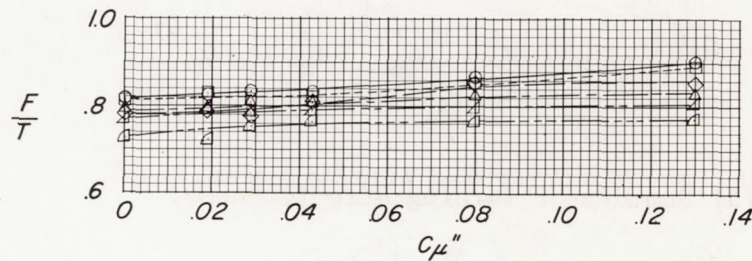


(e) Variation of ratio of power in blowing system to power in slipstream with turning angle.

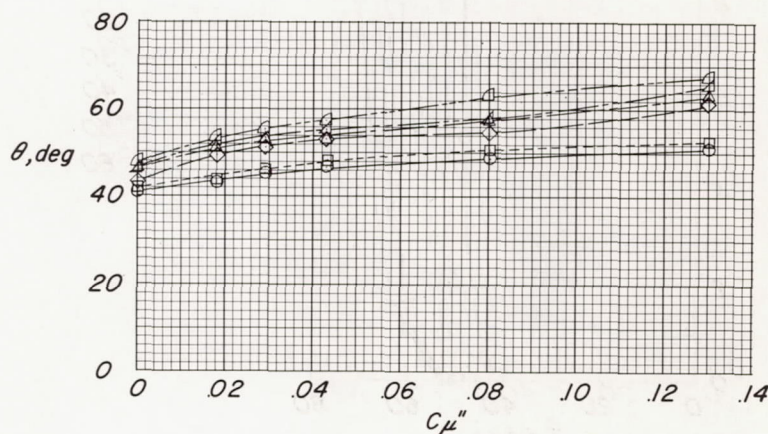
Figure 7.- Concluded.



(a) Pitching moment.

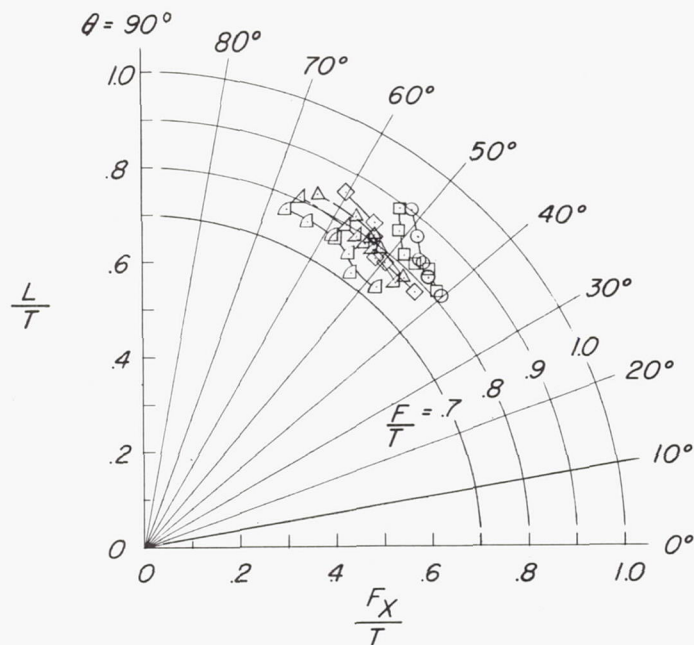


(b) Ratio of resultant force to thrust.

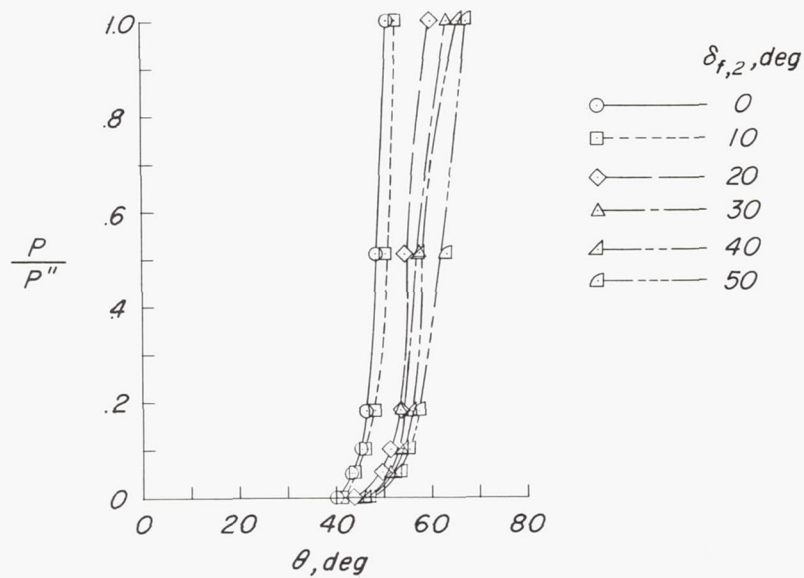


(c) Turning angle.

Figure 8.- Effect of blowing over the flap with $\delta_{f,1}$ constant at 60°
on the model characteristics. $h/D \approx \infty$.

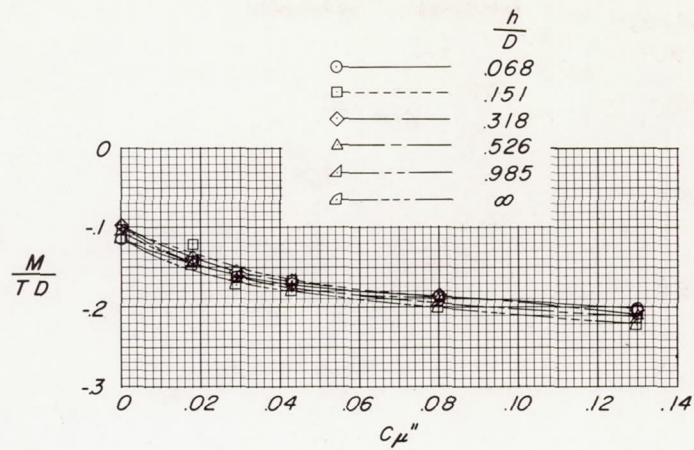


(d) Summary of turning effectiveness.

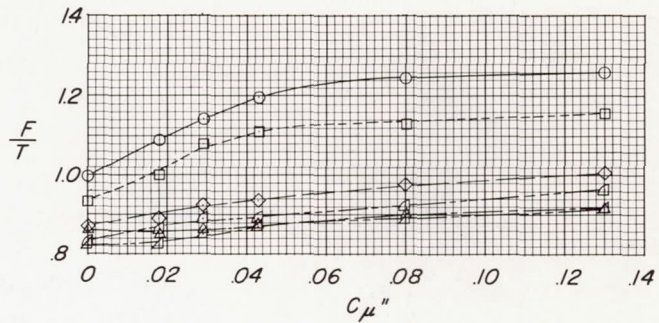


(e) Variation of ratio of power in blowing system to power in slipstream with turning angle.

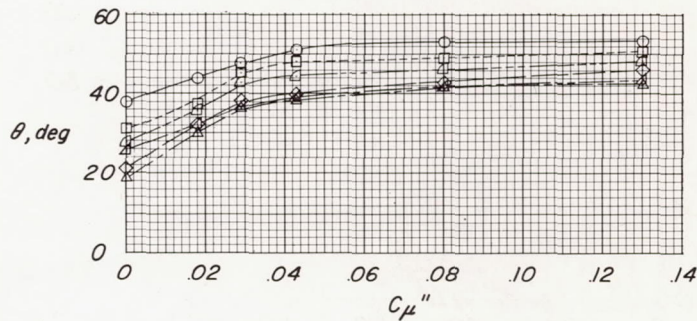
Figure 8.- Concluded.



(a) Pitching moment.

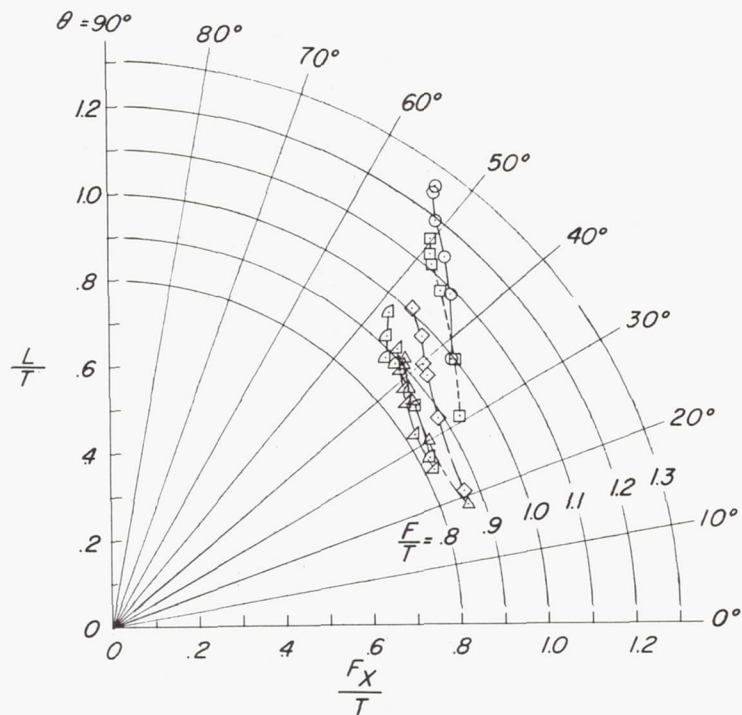


(b) Ratio of resultant force to thrust.

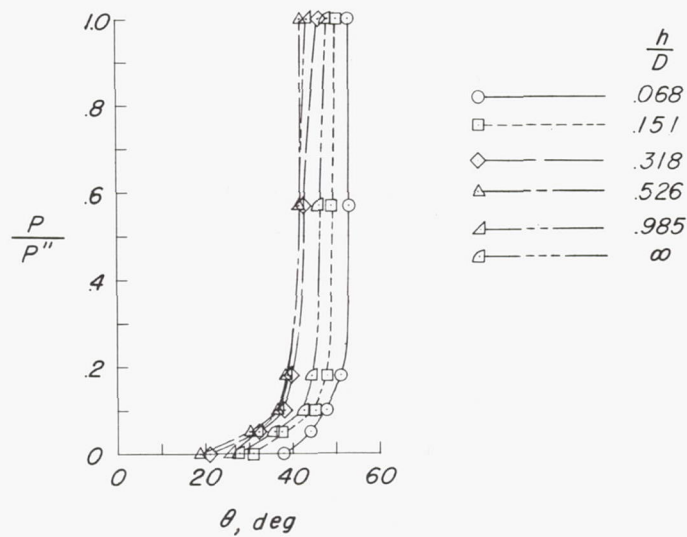


(c) Turning angle.

Figure 9.- Effect of height above the ground and blowing over the flap on the model characteristics. $\delta_{f,1} = 0^\circ$; $\delta_{f,2} = 60^\circ$.

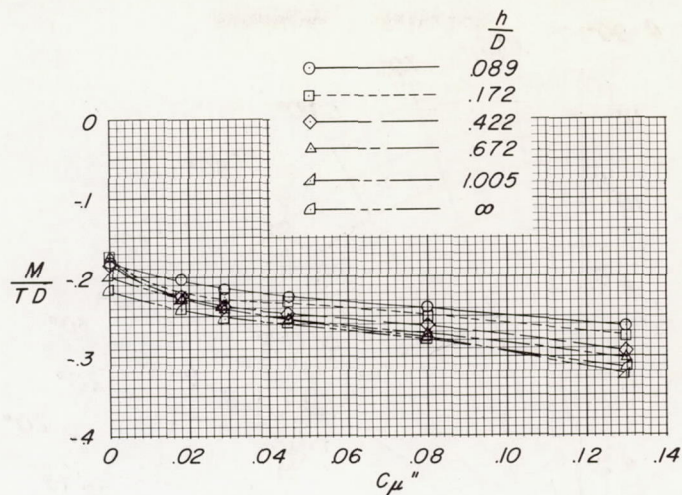


(d) Summary of turning effectiveness.

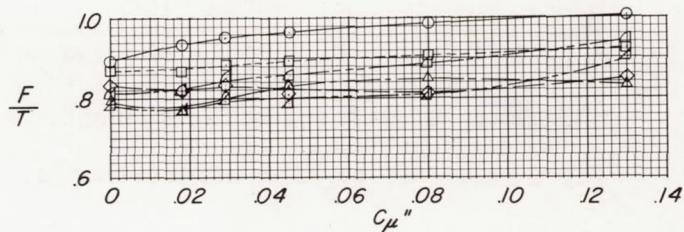


(e) Variation of ratio of power in blowing system to power in slipstream with turning angle.

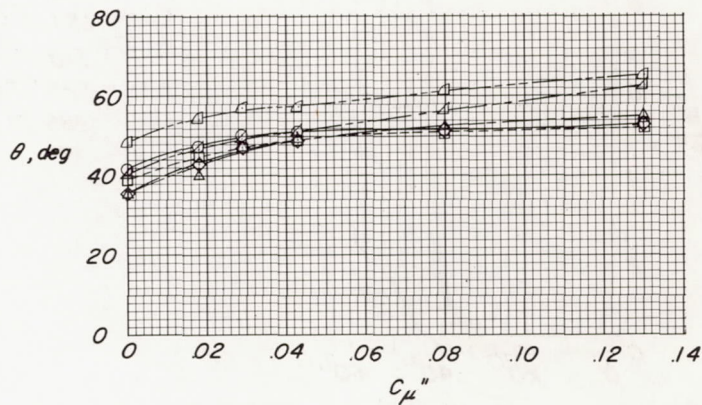
Figure 9.- Concluded.



(a) Pitching moment.

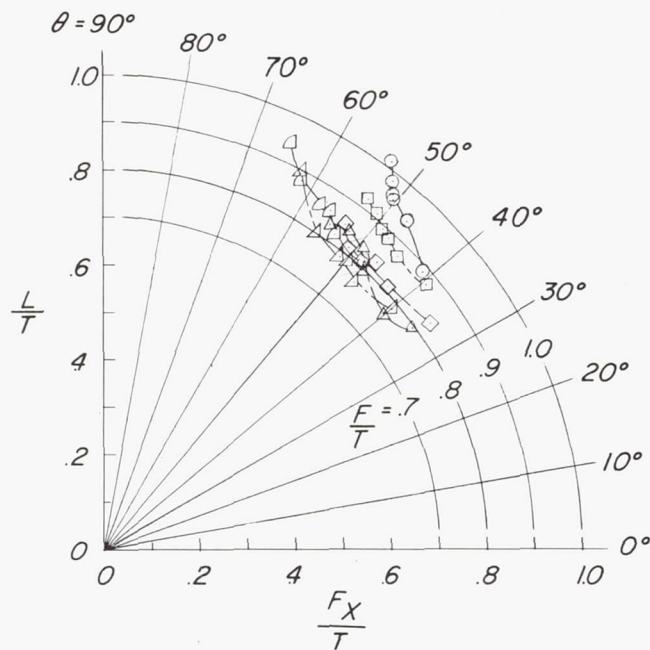


(b) Ratio of resultant force to thrust.

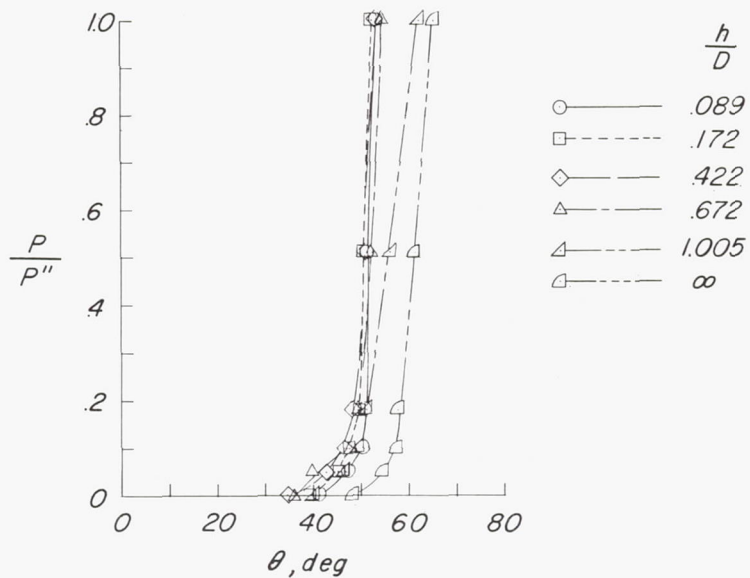


(c) Turning angle.

Figure 10.- Effect of height above the ground and blowing over the flap on the model characteristics. $\delta_{f,1} = 40^\circ$; $\delta_{f,2} = 40^\circ$.

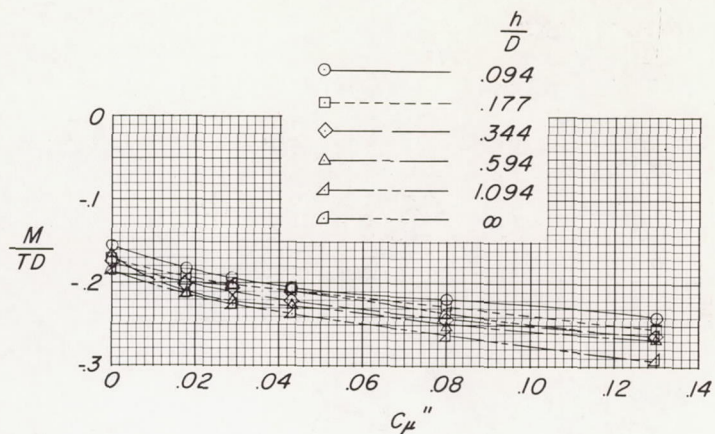


(d) Summary of turning effectiveness.

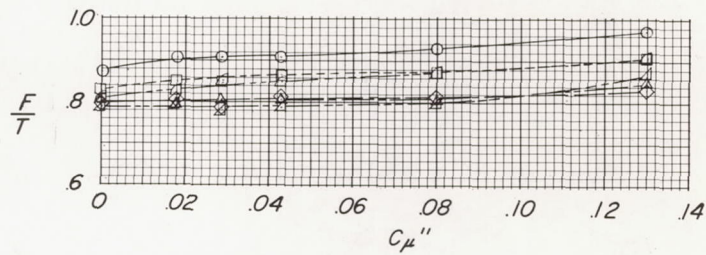


(e) Variation of ratio of power in blowing system to power in slipstream with turning angle.

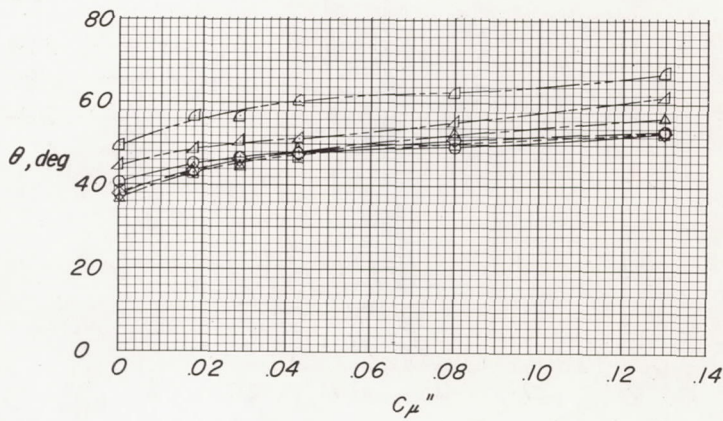
Figure 10.- Concluded.



(a) Pitching moment.

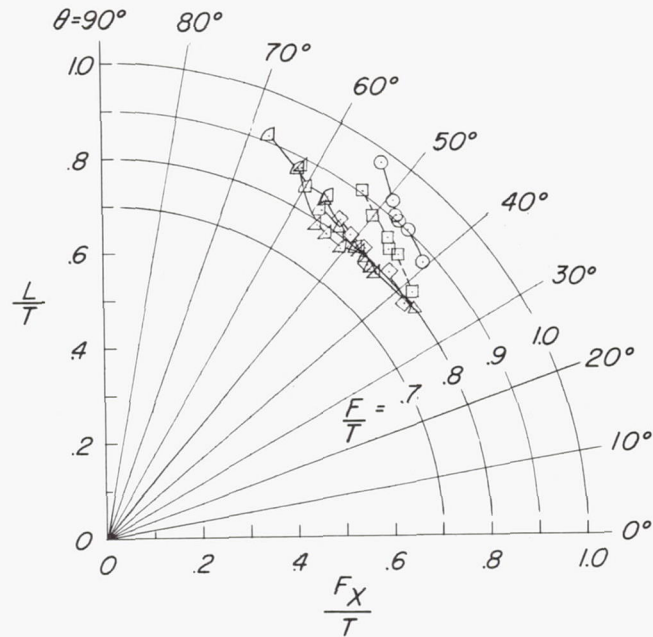


(b) Ratio of resultant force to thrust.

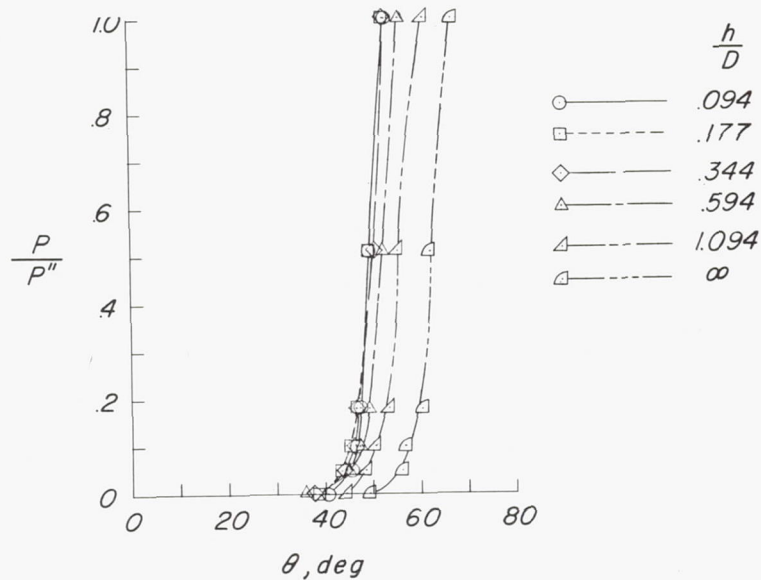


(c) Turning angle.

Figure 11.- Effect of height above the ground and blowing over the flap on the model characteristics. $\delta_{f,1} = 50^\circ$; $\delta_{f,2} = 30^\circ$.

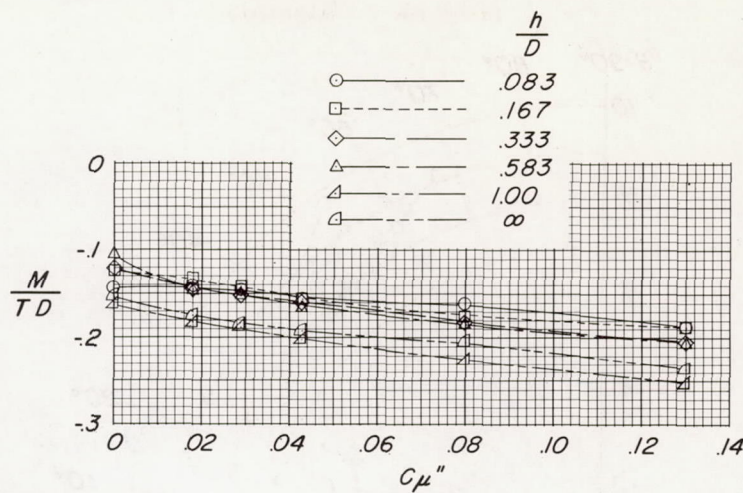


(d) Summary of turning effectiveness.

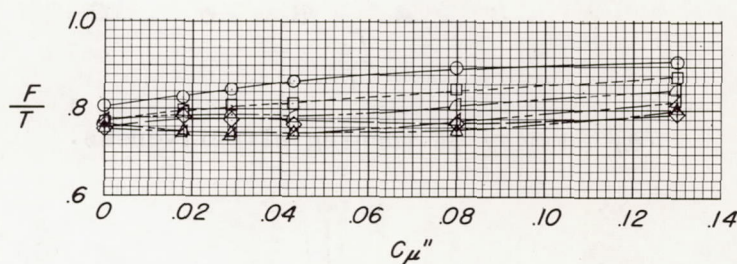


(e) Variation of ratio of power in blowing system to power in slipstream with turning angle.

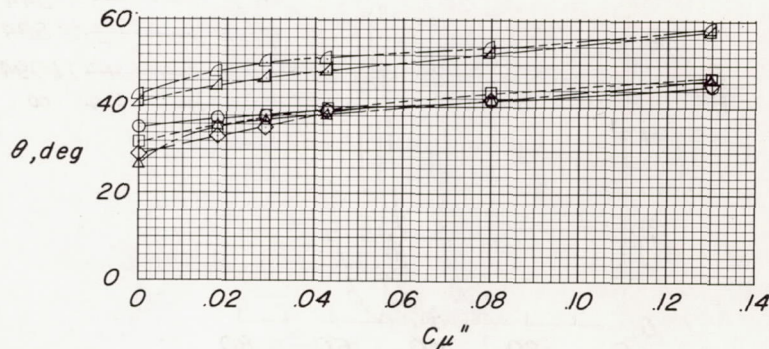
Figure 11.- Concluded.



(a) Pitching moment.

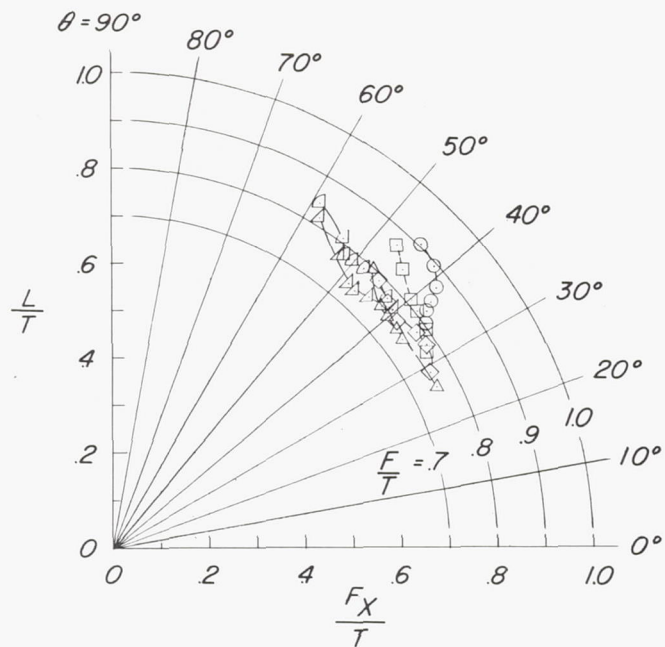


(b) Ratio of resultant force to thrust.

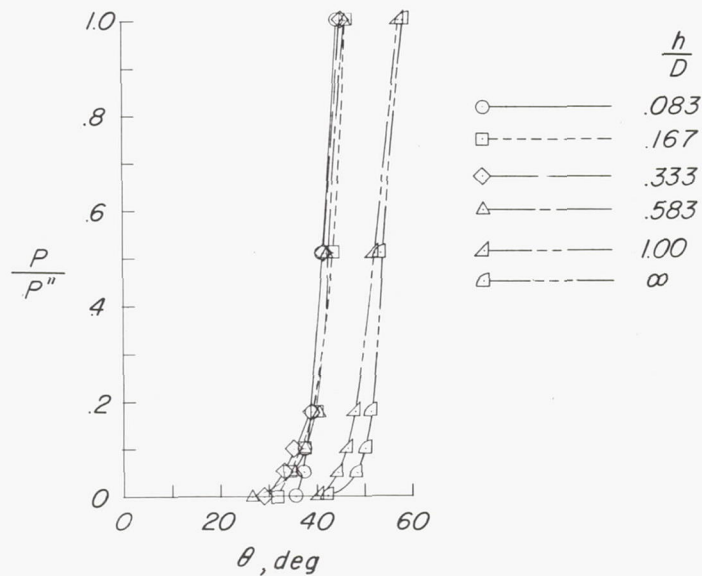


(c) Turning angle.

Figure 12.- Effect of height above the ground and blowing over the flap on the model characteristics. $\delta_{f,1} = 60^\circ$; $\delta_{f,2} = 20^\circ$.

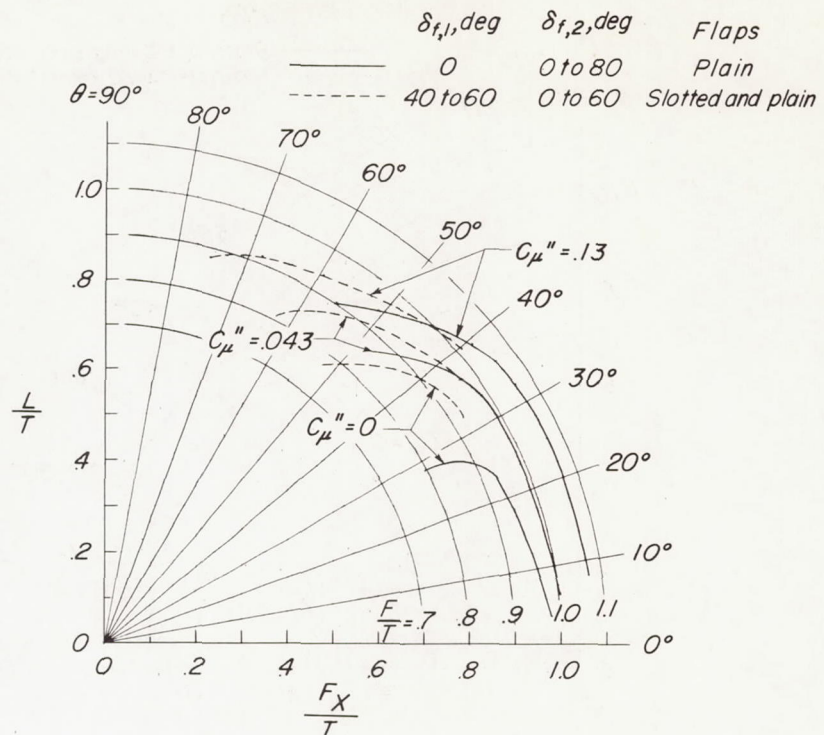


(d) Summary of turning effectiveness.

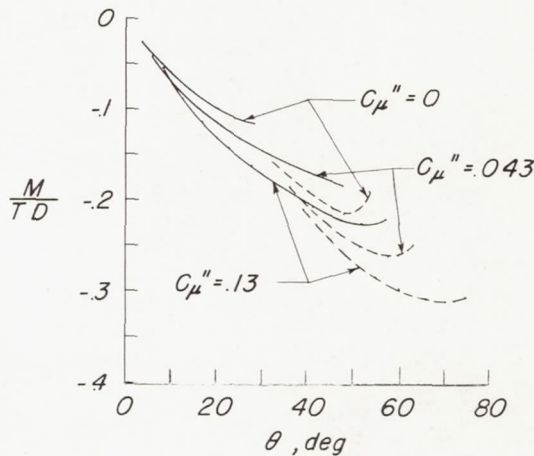


(e) Variation of ratio of power in blowing system to power in slipstream with turning angle.

Figure 12.- Concluded.

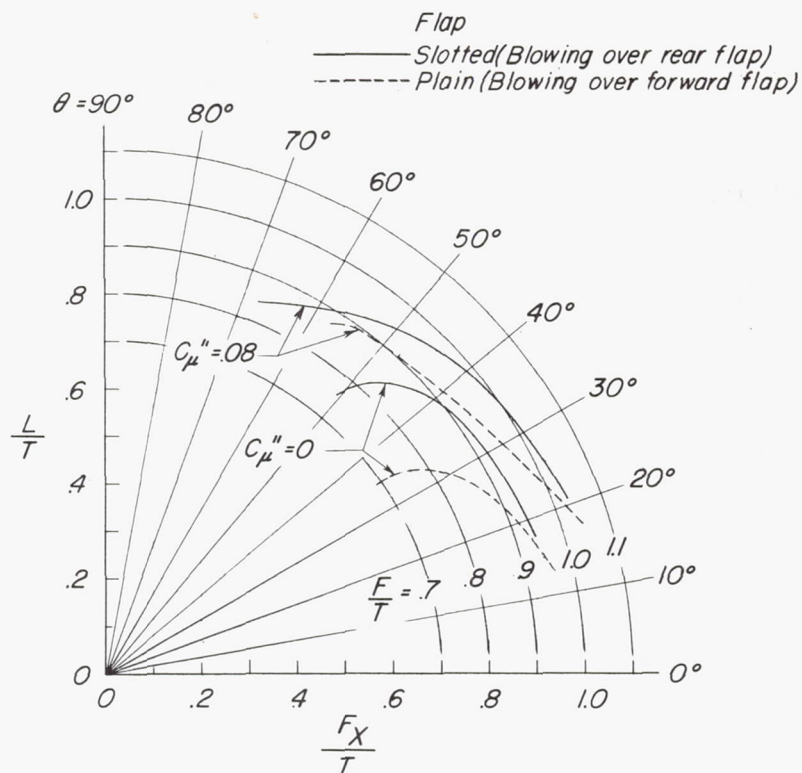


(a) Summary of turning effectiveness.

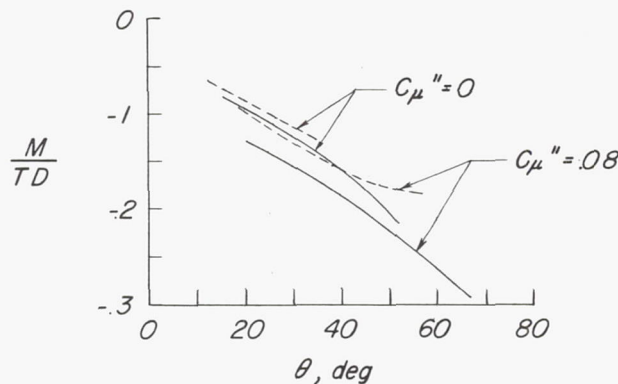


(b) Pitching moment.

Figure 13.- Comparison of the effects of the slotted flap and plain rear flap, with and without blowing over the plain flap, on the turning angle and ratio of resultant force to thrust and diving moments.
 $h/D \approx \infty$.



(a) Summary of turning effectiveness.



(b) Pitching moment.

Figure 14.- Envelopes for different flap deflections of turning angle, ratio of resultant force to thrust, and diving moments for the model of this investigation and the plain flapped model of reference 6.
 $h/D \approx \infty$.

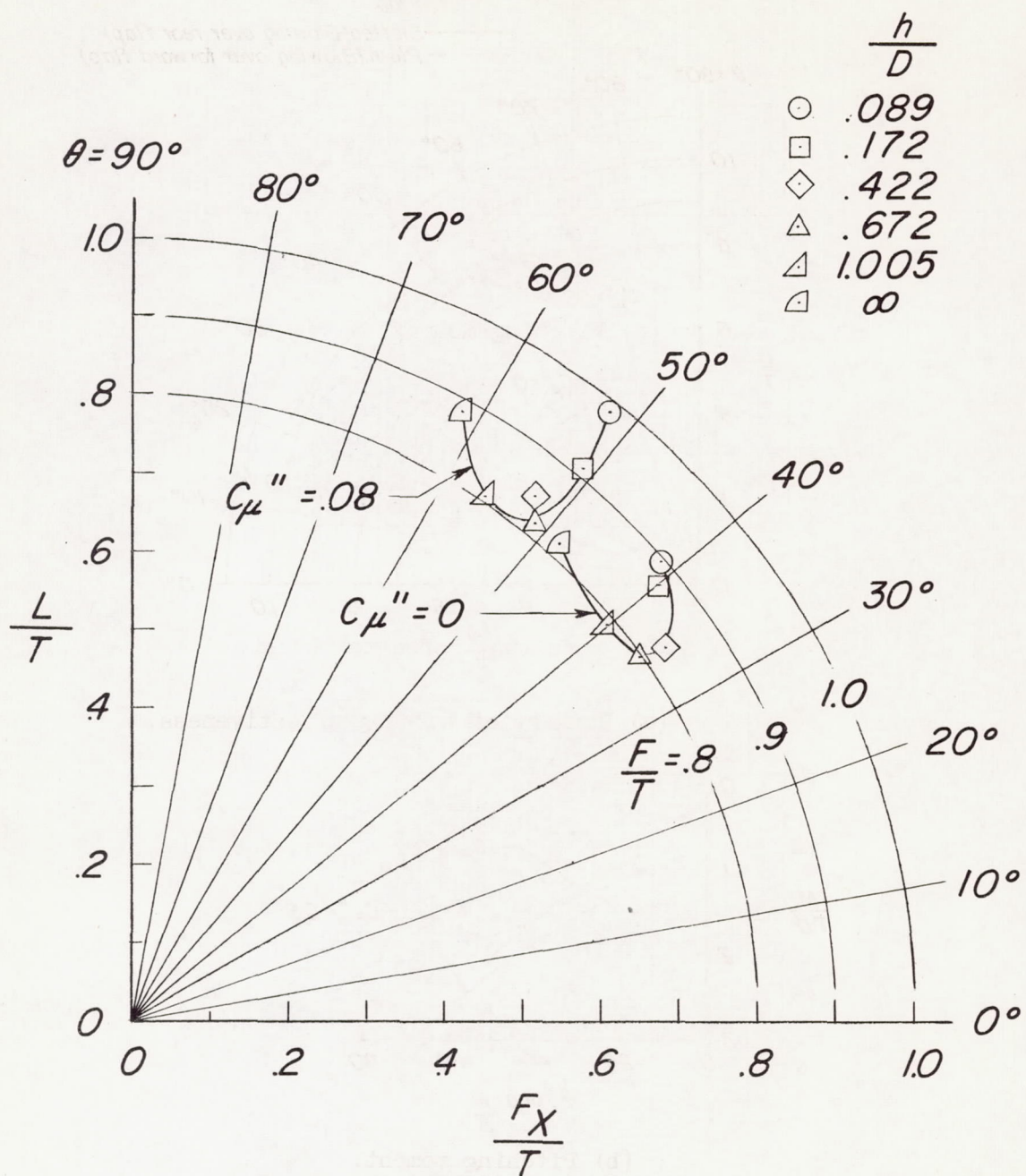
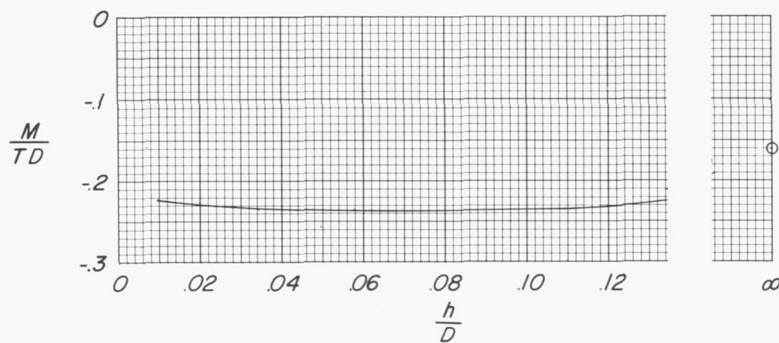
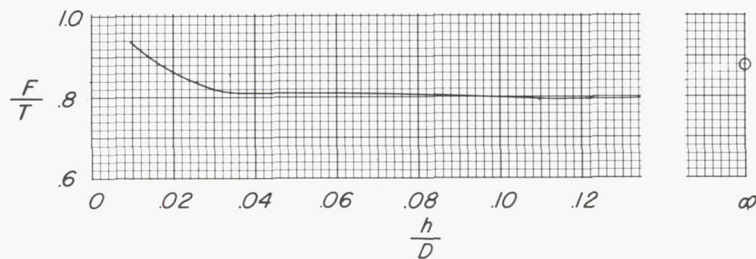


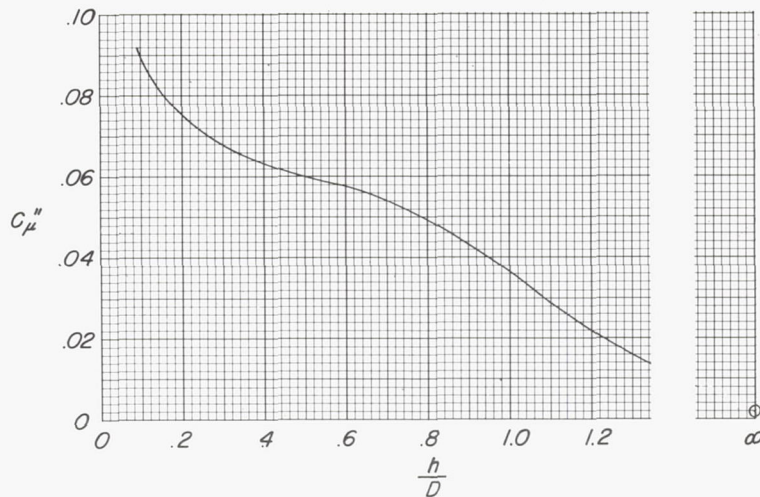
Figure 15.- Effect of ground proximity on the ratio of resultant force to thrust and turning angle. $\delta_{f,1} = 40^\circ$; $\delta_{f,2} = 40^\circ$.



(a) Pitching moment.



(b) Ratio of resultant force to thrust.



(c) Momentum coefficient.

Figure 16.- Variation of pitching moment, ratio of resultant force to thrust, and momentum coefficient required for a constant turning angle of 50° at various heights above the ground.